Engineering Science and Technology, an International Journal 24 (2021) 671–681

HOSTED BY

Contents lists available at ScienceDirect

Engineering Science and Technology, an International Journal

journal homepage: www.elsevier.com/locate/jestch

Simulation and experimental verification of modified sinusoidal pulse width modulation technique for torque ripple attenuation in Brushless DC motor drive

Hetal Patel *, Hina Chandwani

Electrical Engineering Department, Faculty of Technology and Engineering, The Maharaja Sayajirao University of Baroda, Vadodara 390001, Gujarat, India

ARTICLE INFO

Article history:
Received 7 May 2020
Revised 14 August 2020
Accepted 7 November 2020
Available online 3 December 2020

Keywords:
Brushless DC motor
Modified sinusoidal modulation technique
Torque ripple
DC bus utilization
PI controller
ARM controller

ABSTRACT

The Brushless DC motor when operated with120° conduction mode with quasi square wave current in phase with trapezoid back emf leads to finite torque ripple in the commutation region with only two phases conducting at any time. To overcome this, the BLDC motor phases can be supplied with sinusoidal currents which reduce the voltage required to deal with the phase inductance instead of quasi square currents as the change in currents is smoother because of its shape. The proposed technique aims to develop closed-loop speed control of BLDC motor using Modified Sinusoidal Pulse Width modulation (MSPWM) technique by providing sinusoidal stator currents in synchronism with the trapezoid back emf to reduce the commutation torque ripple with improved dynamic performance. The closed-loop control is accomplished by providing a PI controller for a speed control loop. Hall sensors along with shaft encoder are used for detecting the accurate rotor position and speed. This technique provides a higher DC bus utilization as compared to conventional six-step control with torque ripple reduced up to 50%. To justify it, simulation is performed using MATLAB®/SIMULINK at different speed and load. The experimental verification is carried on a prototype using the STM32F407VG microcontroller with Cortex-M4 32 bit ARM controller. The experimental results validates the closed-loop speed control operation of BLDC motor using MSPWM technique.

1. Introduction

The permanent magnet (PM) motors available in two variants are popularly known as Permanent Magnet Synchronous Motor (PMSM) and Brushless DC Motor (BLDC). These motors had gained popularity in electrical drives owing to the amelioration in semiconductor switches with VLSI technology which makes its operation smooth and provides open path for variable frequency variable speed applications. Both motors have their rotor made up of base metal materials like Samarium Cobalt and Neodymium magnets. The discrepancy between the two lies in the stator winding current and the form of back emf. Vector control techniques are generally used for PMSM motors with sinusoidal currents and back emf to provide constant torque operation and are modelled and implemented using the Park transformation theory. Contrarily, the BLDC motor stator is wound with three phase concentrated winding to produce trapezoid back emf and quasi square wave currents with only two phases conducting at a time. The Clarke transformation or abc reference frame theory is used for its modelling and implementation [1]. Pulsating torque is produced due to quasi square wave currents and non-sinusoidal back emf. The BLDC motors possesses greater torque to weight ratio, improved efficiency due to absence of rotor copper losses and reduced maintenance due to electronic commutation which makes them suitable for applications like electric vehicles, aerospace, medical equipments, textile industries, air conditioners, PC's and many more [2,3]. The only disadvantage for BLDC motor is slow dynamic response and increased torque ripple with reference to PMSM.

To overcome the disadvantages and boost the adaptability of BLDC motor drive many control techniques and approaches have been provided. Halfway during sixties, Kirnnich, Heinrick, and Bowes developed the first modulation technique to bring the output voltage and current of the converter nearer to sine wave. [4] Studied the repercussions of advanced commutation angle on the current harmonics and phase current. The harmonics in the torque along with ripple changes with the commutation angle which can be reduced by choosing appropriate control strategies and improved motor design. A pseudo-dq technique is proposed in

* Corresponding author.
E-mail address: hetal_ramjiwala@yahoo.co.in (H. Patel).
Peer review under responsibility of Karabuk University.

https://doi.org/10.1016/j.jestch.2020.11.003
2215-0986/

[5] for non-sinusoidal back emf BLDC motors to compare the efficiency of the drive as compared to the conventional dq theory for minimizing torque ripple. [6] focused on the modulation index (MI) which is said to be determining factor for the PWM techniques. The maximum MI obtained using sinusoidal PWM (SPWM) technique is 0.785 when a sinusoid reference signal is compared with a ramp signal. A flat toped reference signal whose peak value is less than fundamental can be generated by a adding third harmonic to obtain higher value of MI. [7] suggested the dq axis model of permanent magnet machine by using the concept of extended Park transformation by incorporating arbitrary flux patterns for implementing vector control of non -sinusoid back emf machine to scale back the variation in torque and enhance the pursuance of the drive. [8] incorporated a study on trapezoidal, sinusoidal and field oriented commutation strategies for the BLDC motor and PMSM and optimum performance of the drive can be obtained by selecting the precise commutation strategy for a particular motor type. The BLDC motor when operated with modified sinusoidal PWM technique has 6 N harmonic torque instead of pulsating torque and the torque ripple are reduced up to 50% than conventional six-step control [9]. The closed-loop operation is not discussed which shows poor dynamic response of the drive which limits its application. The BLDC motor operating with any type of back emf whether sinusoidal or trapezoidal, the stator copper loss is increased by 10.2% when operated with quasi square wave currents as compared to the vectorial waveform currents as the RMS value of square wave current is greater than the vectorial currents [10]. [11] pointed out the sinusoidal currents with trapezoidal back emf for BLDC motor are most suitable for high speed operation of the drive. In [12], two different FW-SVCs algorithm in two different synchronous reference frames are discussed and enlightens the pros and cones of both methods. The FW-SVC-$\varphi\tau$ techniques discussed by them also approves that sinusoidal currents with non -sinusoidal back emf provides improved drive performance for BDC motor with increased torque ripple at low speed. The work done in [13] shows that for all ranges of speed, the performance of the drive with sinusoidal supply currents outlays the drive performance using quasi square wave currents. The space vector modulation technique (SVM) is used to produce sinusoidal current to prove the performance improvement of the BLDC motor drive with respect to the conventional operation with square wave current. The paper provides the comparison of sinusoidal currents and square wave current at different speed. [14] suggested a current optimization control over the square wave current control technique in stationary reference frame to mitigate commutation torque ripple. [15] suggested an improved direct torque control (DTC) technique using two-phase and three-phase conduction to minimize the commutation torque ripple. [16] suggested a simple overlap angle strategy for commutation torque ripple minimization using two-phase and three-phase conduction over the six-step DTC and twelve step DTC technique.

Since conventionally BLDC motor is excited with quasi square wave currents, it leads to produce commutation torque ripple due finite inductance of winding during commutation interval. The commutation torque ripple produces adverse effects on motor performance like jerks, unwanted noise, vibrations, etc. In this work, it is attempted to reduce commutation torque ripple using sinusoidal excitation at the same time improve the DC link utilization. Since, the proposed MSPWM technique leads motor control in three-phase conduction mode, it naturally offers three-phase conduction during commutation interval which helps to reduce commutation torque ripple in BLDC motor. The proposed technique aims to develop closed loop speed control of BLDC motor and reduce torque ripple using Modified Sinusoidal Pulse Width modulation (MSPWM) by providing sinusoidal stator currents in synchronism with the trapezoid back emf.

With the aim to improve the dynamic response, the closed-loop operation is proposed in this work. Simultaneously, the effect of sinusoidal excitation on torque ripple is also analyzed. Moreover the proposed technique uses only one PI controller to produce sinusoidal currents which reduces control complexity. The paper discusses and verify the closed-loop operation of the drive by performing simulation using MATLAB/SIMULINK at different speed and load with the MSPWM technique and compare the results with the conventional six-step motor control. An encoder is used to obtain instantaneous rotor position for MSPWM technique and hall sensors are used to detect initial rotor position. The simulation results obtained using both the techniques are compared to prove the effectiveness of the proposed method. To validate the proposed method it is tested on a prototype motor with a shaft encoder at high and low speed.

The paper outlines the discussion of the overall system configuration in section (2) including the modelling of MSPWM technique using MATLAB/SIMULINK with detailed analysis of each blocks which includes: (2.1) modelling of MSPWM for BLDC motor drive (2.2) Delta angle calculation (2.3) Speed control of motor (2.4) Commutation Logic circuit for 3-Φ Inverter. Section (3) includes the Simulation Results and its discussion. (4) includes the Experimental verification of the MSPWM technique implemented on the BLDC motor drive followed by (5) conclusions and references.

2. System configuration

The block diagram is proclaimed in Fig. 1 for the analysis of drive performance using MSPWM technique for the BLDC motor. In this technique, a BLDC motor with trapezoid back emf is operated with sinusoidal currents to generate optimal torque per ampere current.

The three phases of the motor stator winding are supplied through an electronic commutator. The recognition of rotor poles is mandatory for a sensored drive to decide the commutation logic for the three phase stator winding by relevant switching of the inverter switches. Three position sensors with encoder are provided to decode the exact rotor position to generate six commutation states in one electrical cycle. The rotor position and speed are obtained using an encoder. Initially, the motor is started using the status of Hall sensors. The stator flux is changed in accordance with the rotor position. Maximum torque per ampere is produced when the rotor flux follows the stator flux by an angle of 90°. The optimal delta angle (δ) is calculated by transforming the three phase stator currents in to rotating dq axis reference frame from abc reference frame using Park's transformation. The motor speed is calculated from the rotor position and compared with the quoted speed. The difference of the two speeds is fixed by a PI controller. The gain of controller controls the magnitude of the three phase voltages by the virtue of modulation index. Three-phase sinusoidal voltages are generated in the voltage generation block using the delta angle, modulation index and electrical rotor position. Three saddle shape modulating waves are generated which are matched with the triangular carrier wave to engender the gate pulses for the six inverter switches by the PWM modulator block. As variation in speed is in straight proportion to the applied voltage, motor control is inhibited by varying the duty cycle of the gate pulses.

2.1. Mathematical modelling of MSPWM for BLDC drive

For a balanced 3-Φ system, the stator phase currents ia + ib + ic = 0. The dynamic voltage equations of BLDC motor with trapezoidal back emf is obtained from the inductance matrix as given in (1).

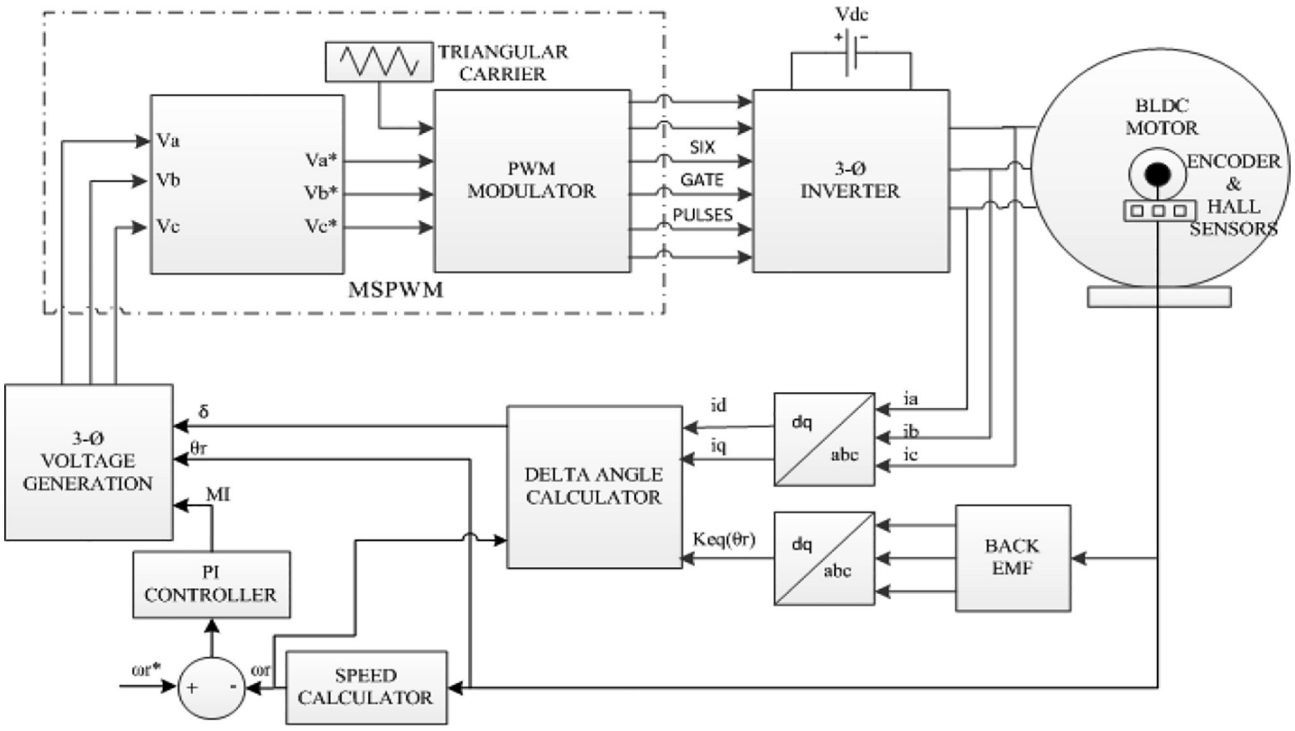

Fig. 1. Schematic block diagram of overall system.

$$\begin{bmatrix} Va \\ Vb \\ Vc \end{bmatrix} = r_s \begin{bmatrix} 1 & 0 & 0 \\ 0 & 1 & 0 \\ 0 & 0 & 1 \end{bmatrix} \begin{bmatrix} ia \\ ib \\ ic \end{bmatrix} + \begin{bmatrix} L-M & 0 & 0 \\ 0 & L-M & 0 \\ 0 & 0 & L-M \end{bmatrix} \frac{d}{dt} \begin{bmatrix} ia \\ ib \\ ic \end{bmatrix} + \begin{bmatrix} ea \\ eb \\ ec \end{bmatrix} \quad (1)$$

where,
V_a, V_b, V_c = stator phase voltages
i_a, i_b, i_c = stator phase currents
e_a, e_b, e_c = trapezoidal phase back emf
r_s = stator resistance per phase
L_s = stator inductance per phase,
M = mutual inductance
$\psi_{abc} = L_s i_{abc}$ = stator flux linkage

For permanent magnet machine with trapezoidal back emf as expressed in (2) are function of rotor position, rotor speed and back emf constant.

$$\begin{aligned} e_a &= \omega_r \kappa_e(\theta_r) \\ e_b &= \omega_r \kappa_e(\theta_r - 2\pi/3) \\ e_c &= \omega_r \kappa_e(\theta_r + 2\pi/3) \end{aligned} \quad (2)$$

The back emf constant K_e depends on the winding flux linkages imposed by the permanent magnet and rotor position.

$$\kappa_e(\theta_r) = \frac{d\psi(\theta_r)}{d\theta_r} \quad (3)$$

The electromagnetic torque is expressed as in (4)

$$T_e = \frac{(e_a i_a + e_b i_b + e_c i_c)}{\omega_m} (Nm) \quad (4)$$

Equation (5) is expressed in terms of electromagnetic torque, load torque, inertia J, friction coefficient B widely known as motion equation

$$Te - T_l = \frac{Jd\omega_m}{dt} + B \quad (5)$$

Differentiation of rotor position w.r.t time gives rotor speed in as shown in (6)

$$\frac{d\theta_r}{dt} = \frac{p}{2}\omega_m \quad (6)$$

$$\theta_r = \int \omega_r dt$$

To realize the six commutation instances, three hall sensors are incorporated in the stator such that when they are covered by magnetic "N" pole they conduct. Maximum two hall sensors are covered by "N" Pole and at least one hall sensor remains under the influence of "N" pole at any time [17]. Table 1 shows the hall sensor output and switching states of 3-Φ inverter bridge to provide excitation to the three phase stator winding for the rotor position.

Intending to obtain sine currents, dq transformation of all the variables defined in the abc reference frame is carried out using Park transformation. The dynamic equations of BLDC motor described in Eqs. (1) to (6) are transformed in the dq reference frame using Eqs. (7) to (12).

$$(f_{qdos})^T = [f_{qs} f_{ds} f_{os}] \quad (7)$$

$$(f_{abcs})^T = [f_{as} f_{bs} f_{cs}] \quad (8)$$

$$(f_{qdos})^T = K_s (f_{abcs})^T \quad (9)$$

$$K_s = \frac{2}{3} \begin{bmatrix} \cos\theta_r & \cos(\theta_r - 2\pi/3) & \cos(\theta_r + 2\pi/3) \\ \sin\theta_r & \sin(\theta_r - 2\pi/3) & \sin(\theta_r + 2\pi/3) \\ 1/2 & 1/2 & 1/2 \end{bmatrix} \quad (10)$$

Table 1
Hall sensor output and inverter switching states.

H_a	H_b	H_c	S1	S2	S3	S4	S5	S6
1	0	1	1	–	–	1	–	–
1	0	0	1	–	–	–	–	1
1	1	0	–	–	1	–	–	1
0	1	0	–	1	1	–	–	–
0	1	1	–	1	–	–	1	–
0	0	1	–	–	–	1	1	–

$$\begin{bmatrix} f_{ds} \\ f_{qs} \\ f_{os} \end{bmatrix} = \frac{2}{3}\begin{bmatrix} \cos\theta_r & \cos(\theta_r - 2\pi/3) & \cos(\theta_r + 2\pi/3) \\ \sin\theta_r & \sin(\theta_r - 2\pi/3) & \sin(\theta_r + 2\pi/3) \\ 1/2 & 1/2 & 1/2 \end{bmatrix}\begin{bmatrix} f_{as} \\ f_{bs} \\ f_{cs} \end{bmatrix} \tag{11}$$

$$(\psi_{dqos})^T = [\psi_{ds} - \psi_{qs}0] \tag{12}$$

In above equation parameter f can be a voltage, current or flux linkage. The zero sequence components are neglected for balanced three phase system.

The stator currents in abc frame are transformed in rotating reference frame fixed on the rotor using Park transformation to get rid of the time varying inductances. The dynamic equations after applying the dq transformation can be expressed as below. As the rotor rotates, the angle (θ_r) between the rotor and stator axis changes [18,19] as shown in Fig. 2. A shaft encoder is used to obtain the angle (θ_r) between the stator magnetic field and rotor magnetic field.

To achieve optimum torque, it is necessary to control the q axis current (i_q) and d axis current (i_d). The current requirement to produce maximum torque is lessen by maximal torque per ampere (MTPA) technique which minimize the stator copper losses and maximize the efficiency of motor [9,10]

$$V_{ds}^r = r_s i_{ds}^r + p\psi_{ds}^r - \omega_r \psi_{qs}^r + \omega_r K_{ed}^r(\theta_r) \tag{13}$$

$$V_{qs}^r = r_s i_{qs}^r + p\psi_{qs}^r + \omega_r \psi_{ds}^r + \omega_r K_{eq}^r(\theta_r) \tag{14}$$

$$\psi_{ds}^r = L_d i_{ds}^r \tag{15}$$

$$\psi_{qs}^r = L_q i_{qs}^r \tag{16}$$

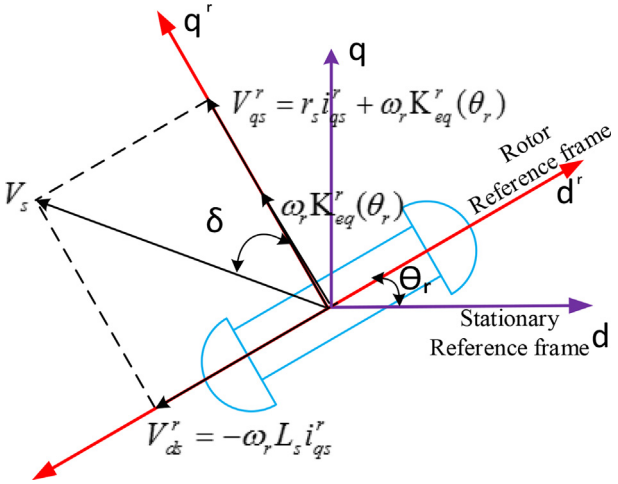

Fig. 2. Voltage vector representation.

Considering the BLDC motor with non -salient poles (Lq = Ld = Ls) helps to simplify above expressions

$$L_q = L_d = L_s \tag{17}$$

$$\begin{bmatrix} V_{ds}^r \\ V_{qs}^r \end{bmatrix} = \begin{bmatrix} r_s + p\psi_{ds}^r & -\omega_r L_s \\ \omega_r L_s & r_s + p\psi_{qs}^r \end{bmatrix}\begin{bmatrix} i_{ds}^r \\ i_{qs}^r \end{bmatrix} + \omega_r \begin{bmatrix} K_{ed}^r(\theta_r) \\ K_{eq}^r(\theta_r) \end{bmatrix} \tag{18}$$

$$T_{em} = \frac{3}{2}\frac{p}{2}(\psi_{ds}^r i_{ds}^r - \psi_{qs}^r i_{qs}^r) \tag{19}$$

2.2. Delta angle calculation

For non-salient machines, optimal torque is obtained from the q-axis current and hence the d axis current is considered to be zero in Eqs. (13) to (19) for a surface mounted BLDC motor with salient pole rotor as the reluctance torque is not developed. At the same time when the motor is operated with MTPA using MSPWM technique, sinusoidal stator current are produced which reduces the stator copper losses [9,10]. The voltage and electromagnetic torque equations are modified as shown in below equations.

$$V_{ds}^r = -\omega_r L_s i_{qs}^r \tag{20}$$

$$V_{qs}^r = r_s i_{qs}^r + \omega_r K_{eq}^r(\theta_r) \tag{21}$$

$$T_{em} = \frac{3}{2}\frac{p}{2}(\psi_{qs}^r i_{qs}^r) \tag{22}$$

From Eq. (22) it can be observed that the motor electromagnetic torque is directly controlled by the quadrature axis current [20]. For accurate control of BLDC motor drive, the stator currents should be in synchronism with the back emfs. Since the back emfs is function of theta displaced with reference to stator magnetic field, it is necessary to determine the angle between stator field and rotor field. This angle is known as delta angle or displacement angle. In order to implement MSPWM technique, a optimal delta angle (δ) is obtained using (23).

$$\delta = \tan^{-1}\left(\frac{\omega_r L_s i_{qs}^r}{r_s i_{qs}^r + \omega_r K_{eq}^r(\theta_r)}\right) \tag{23}$$

2.3. Speed control of BLDC motor drive

The control of speed in the BLDC motor drive is realized by controlling the duty ratio of the six gate pulses fed to the 3-Φ VSI which in turn regulates the DC bus voltage. For this a PI controller is used as it is resilient and most trusted controller.

$$MI = K_p e(t) + K_i \int e(t)d(t) \tag{24}$$

where,
MI = Modulation Index
e(t) = error signal of speed

K_p = proportionality gain
K_i = integral gain

The actual motor speed obtained from an encoder is mapped with the set speed. The difference of the two is processed by the PI controller. The controlled output signal thus obtained which is Modulation Index (MI) here, is used to generate three phase sinusoidal voltages. The three reference modulating signals are generated so as to improve the modulation index as compared to sinusoidal PWM technique. These modulating signals are processed in PWM modulator block which compares them with high frequency carrier wave to produced six gate pulses. The maximum output is obtained by changing the duty ratio to unity. The implemented speed control method is simple and does not require hysteresis controllers, sector selector or torque estimator which reduces the complexity of the overall system. The added advantage of this method is reduced torque ripple as compared to sinusoidal pulse width modulation technique as well as six-step control.

2.4. Commutation logic circuit

In BLDC motor drive, the 3-Φ VSI acts like an electronic commutator which supply three phase current in accurate dimensions with the rotor position to produce required torque. For this, three phase terminal voltages are generated based on the modulation index, inverter pole voltage and the modulating signal as given in (25).

$$V_a = \frac{V_{dc}}{2} * MI * \mathrm{Sin}\left(\theta_r + \delta + \frac{\pi}{2}\right)$$

$$V_b = \frac{V_{dc}}{2} * MI * \mathrm{Sin}\left(\theta_r - \frac{2\pi}{3} + \delta + \frac{\pi}{2}\right)$$

$$V_c = \frac{V_{dc}}{2} * MI * \mathrm{Sin}\left(\theta_r + \frac{2\pi}{3} + \delta + \frac{\pi}{2}\right) \quad (25)$$

The rotor angle δ is estimated using machine parameters, speed measured using encoder, dq axis current and back emf constant ($K^{E}_{eq}(\theta_r)$); where θ_r is calculated from Eq. (6). The initial rotor position is obtained using hall sensors.

In sinusoidal pulse width modulation technique, three sine reference waves are compared with the triangular waves to generate gate pulses. Modulation index (MI) is the relation between the peak magnitudes of the modulating waveform and the carrier waveform. It relates the voltage of DC link and the magnitude of pole voltage (fundamental component) output by the inverter. The value of MI determines the pulse width of the average pole voltage. It varies between 0 < MI < 1.

In modified SPWM three saddle shape modulating signals are generated using Eq. (26) which is compared with the triangular carrier wave which increases the inverter output voltage by 15% which improves the DC bus voltage utilization. The min (Va,Vb, Vc) indicates instantaneous minimum values of the three phase voltages.

$$\mathrm{Va}^* = V_a - \min(V_a, V_b, V_c)$$

$$\mathrm{Vb}^* = V_b - \min(V_a, V_b, V_c)$$

$$\mathrm{Vc}^* = V_c - \min(V_a, V_b, V_c) \quad (26)$$

The flow chart shown in Fig. 3 gives the overview of the operation of BLDC motor drive using MSPWM technique. The various parameters like current; voltage; torque and theta are calculated from the MSPWM inverter fed BLDC motor. The rotor position is obtained using an encoder. The abc to dq transformation is applied to measured current and back emf to calculate the value of delta angle for obtaining three phase voltages and sinusoidal currents.

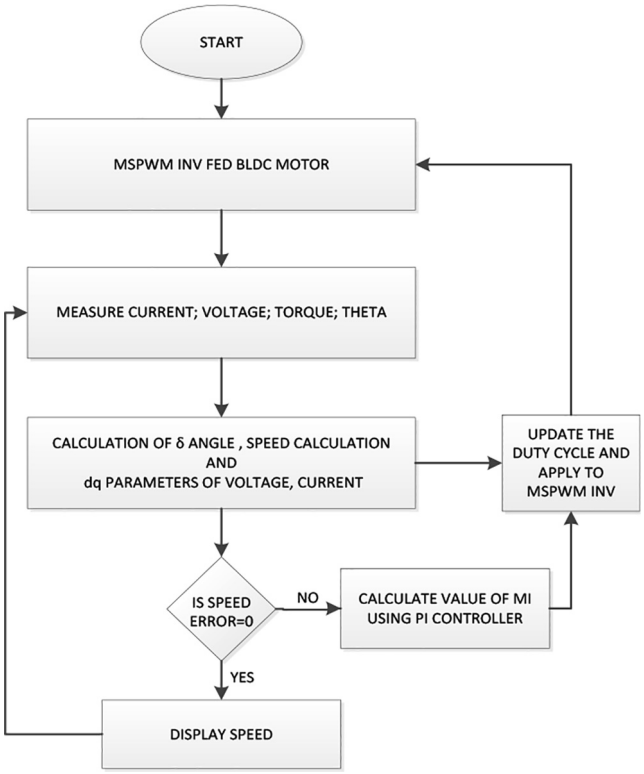

Fig. 3. Flow chart for closed-loop control of BLDC motor using MSPWM technique.

The desired speed is calculated which is compared with the set speed using PI controller. If the error is zero, the actual speed is maintained and displayed. If the error is not equal to zero, the PI controller sets the appropriate modulation index to bring the error to zero by adjusting the duty cycle of the PWM pulses fed to the inverter.

3. Simulation results

The realization of the MSPWM technique is carried in MATLAB/SIMULINK environment with the aim of obtaining improved BLDC motor performance as compared to conventional six-step operation. The BLDC motor is tested at different speed and load. The results of the proposed technique are compared with conventional six-step control at lower speed and higher speed. Comparison between the six-step control technique and the MSPWM technique is shown at a speed of 2500 rpm with 5 Nm load in Fig. 4a) and Fig. 4(b) respectively. The conventional technique produces quasi square wave stator current in phase with the trapezoid back emf producing large torque ripple due to the mismatch in the slope of rising current and decaying current with two phases conducting at any time. With MSPWM technique, a sinusoidal current is produced in phase with the motor trapezoidal back. It can also be observed that the duty ratio is increased resulting in improved DC bus utilization using the proposed technique. The ripple in the torque with the MSPWM technique is comparatively less at same speed and applied load which leads to improved drive operation. Comparing Fig. 4(b) and (c) it can be noticed that at same speed with an applied load torque reduced to 2.5 Nm the current is halved. Fig. 5 (a) and (b) shows the motor operation at a speed of 1750 rpm with a load of 5 Nm and 2.5 Nm.

It can be noticed that if speed is made constant and load is reduced by half, the motor current is reduced proportionately. In

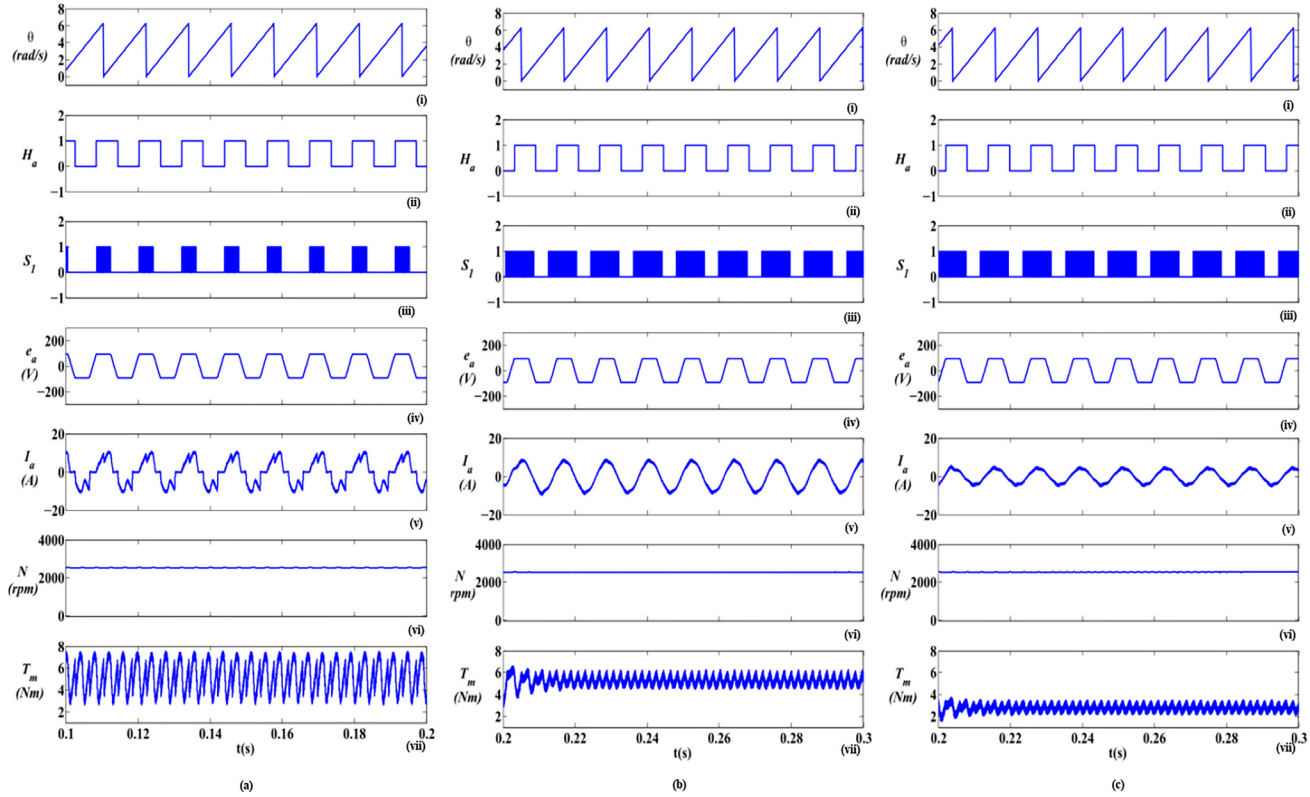

Fig. 4. Performance comparison of BLDC motor with (a) Conventional Six-step control technique at a speed of 2500 rpm with applied load of 5 Nm (b) MSPWM technique at a speed of 2500 rpm with applied load of 5 Nm (c) MSPWM technique at a speed of 2500 rpm with applied load of 2.5 Nm showing (i) rotor position (θ) (ii) hall output (Ha) (iii) gate pulses to switch S1 (iv) motor back emf (ea) (v) stator current (Ia) (vi) speed (N) (vii) motor torque (Tm).

Fig. 5c) and (d), the motor speed is increased to 3000 rpm with the same applied load As speed is increased there is an increase in stator voltage and the modulating voltage. The torque ripple seems to be reduced at higher speed. Similarly a comparison is shown of MSPWM technique with six-step control at a speed of 3000 rpm and 2.5 Nm load in Fig. 6(a) and Fig. 6(b) which proves increased duty ratio and DC bus utilization with reduced torque ripple. Perfect tuning of the PI controller leads the motor to operate at the set speed.

A comparative analysis of torque ripple under steady state at different speed and loading condition with MSPWM technique and conventional six-step control as obtained from the simulation results shown in Fig. 7. It can be observed that, with quasi square wave currents, the torque waveforms with conventional six-step control has sharp notches in the commutation region as compared to the MSPWM technique which provides smooth torque curve with sinusoidal currents. At a speed of 1750 rpm some steady state error in speed is observed with six-step control. The torque ripple and ripple factor obtained from the waveforms at different speed and load for both methods is tabulated in Tables 2 and 3.

From above comparison it can be observed that with the MSPWM technique, the torque ripples are reduced up to 50% than the conventional six-step control. The comparison shows improved drive performance at different speed and load with the proposed technique.

4. Experimental verification

In order to verify the MSPWM technique simulation results experiment is performed on different speeds above and below the rated speed. A voltage control loop is used to perform the experiment using the MSPWM technique to control the speed of motor with different load condition. The overall system requirement for hardware implementation is as shown in Fig. 8. The prototype consist of a 36 V, 4 pole BLDC motor with parameters listed in Table 4 with a loading arrangement, STM32F407VG ARM controller discovery card with a clock frequency of 168 MHz, a three phase voltage source inverter (VSI) with six insulated gate bipolar transistors (IGBTs), motor current sensor card, an intelligent IGBT driver card is provided to quarantine the low voltage controller circuit and high voltage power circuit, DC power circuit for the controller, driver card and inverter circuit. The rating of the motor is as given in Appendix. To generate the six gate pulses for six inverter switches, advanced Timer-8 is utilized. To prevent the shoot through fault a dead band of 1 micro second is provided. The value of switching frequency is 10 kHz, the sampling frequency of inner loop quantities is 25 kHz and outer speed loop operates at 2.5 kHz. The set speed and actual speed is displayed on the LCD display. The hardware results are captured using 4channel Digital Signal Oscilloscope. The speed control loop is incorporated using a PI controller to process the error signal generated from the comparison between the reference speed and calculated speed. The 1250ppr inbuilt shaft encoder used to calculate speed is given to the A9 and E9 pin to timer 1 of the controller card. A shift in speed from 1500 rpm to 1000 rpm and then from 1000 rpm to 1500 rpm is applied to witness the motor behaviour at constant load and with applied load change. The accurate tuning of PI controller has leaded the drive to follow reference speed. A belt and pulley arrangement is provided for loading the motor. The loading is provided by increasing the tension on the belt. A maximum loading of 2.5 A can be provided for the given motor.

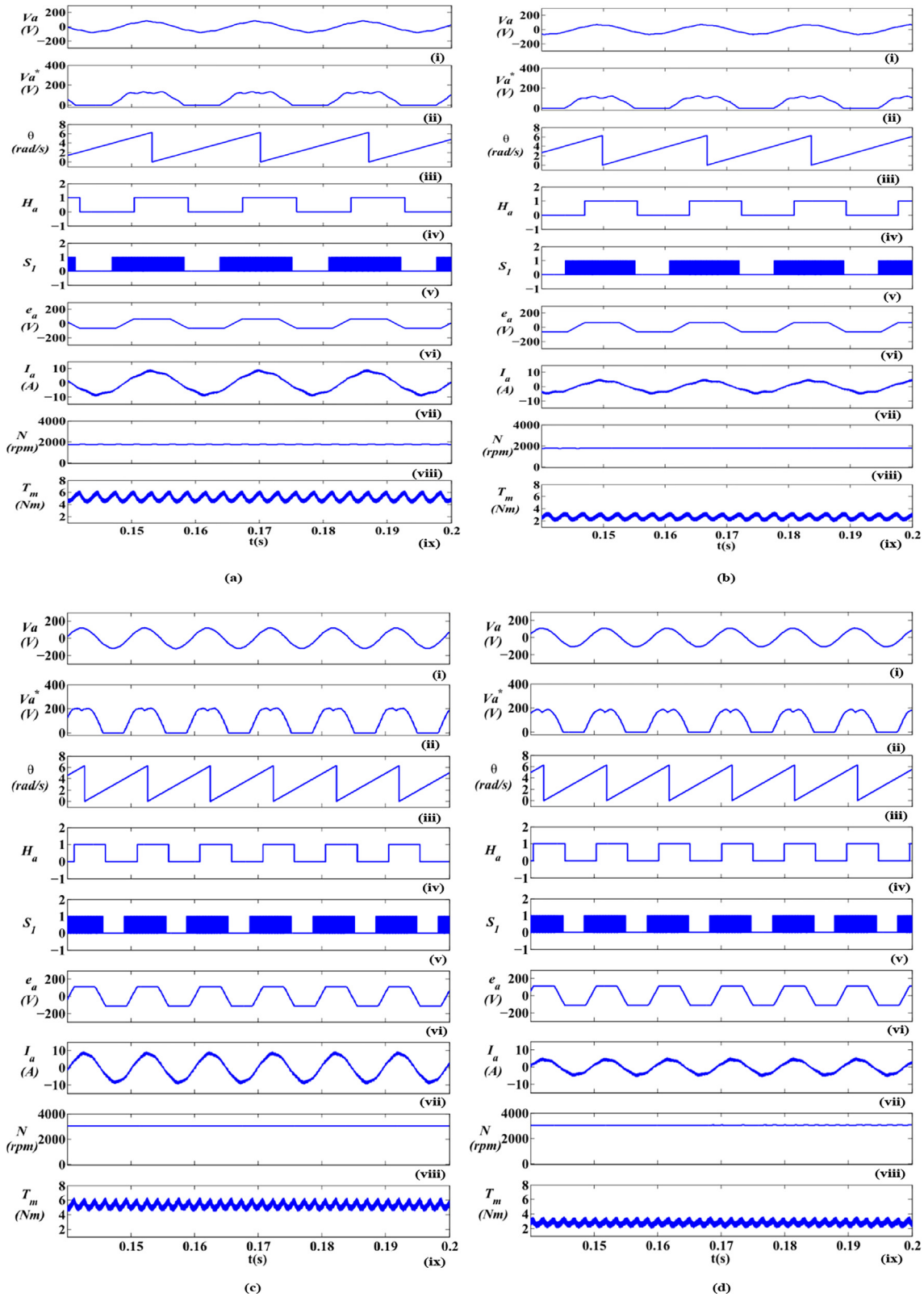

Fig. 5. Performance comparison of BLDC motor with MSPWM technique (a) speed of 1750 rpm with applied load of 5 Nm (b) speed of 1750 rpm with applied load of 2.5 Nm (c) speed of 3000 rpm with applied load of 5 Nm (d) speed of 3000 rpm with applied load of 2.5 Nm showing (i) variation of phase voltage (Va) (ii) modulating voltage (Va*) (iii) rotor position (θ) (iv) hall output (Ha) (v) gate pulses for switch S1 (vi) motor back emf (ea) (vii) stator current (Ia) (viii) speed (N) (ix) motor torque (Tm).

The experimental results provide the actual behavior of the presented technique in real time on the BLDC motor drive operation. The conduction period of PWM pulses shows variation with the applied speed change and the response of the stator current and torque to the change in load. From Fig. 9(a) and Fig. 10(a), it can be discovered that, using MSPWM technique a discontinuous type saddled shape modulating signal is generated. The width of modulating reference signal is also increased with the speed.

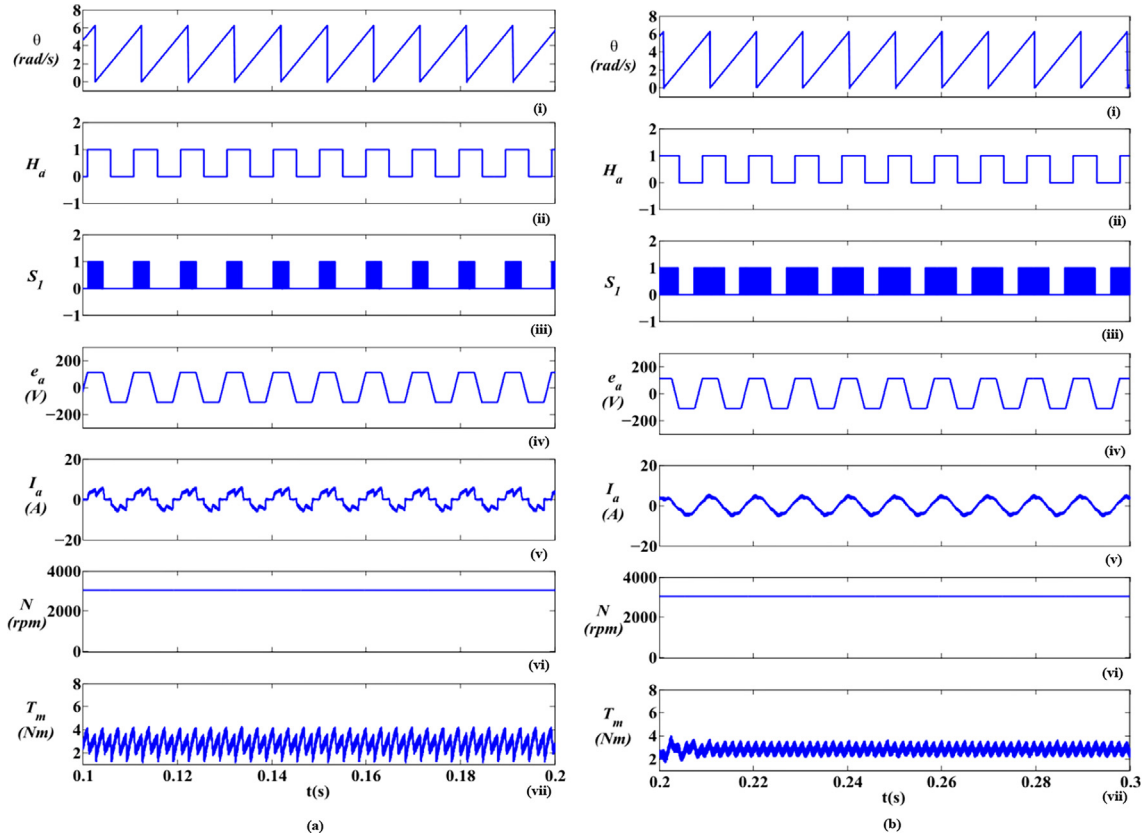

Fig. 6. Performance comparison of BLDC motor with (a) Conventional Six-step Control & (b) MSPWM technique at a speed of 3000 rpm with applied load of 2.5 Nm showing (i) rotor position (θ) (ii) hall output (Ha) (iii) gate pulses to switch S1, (iv) motor back emf (ea) (v) stator current (Ia) (vi) speed (N) (vii) motor torque (Tm).

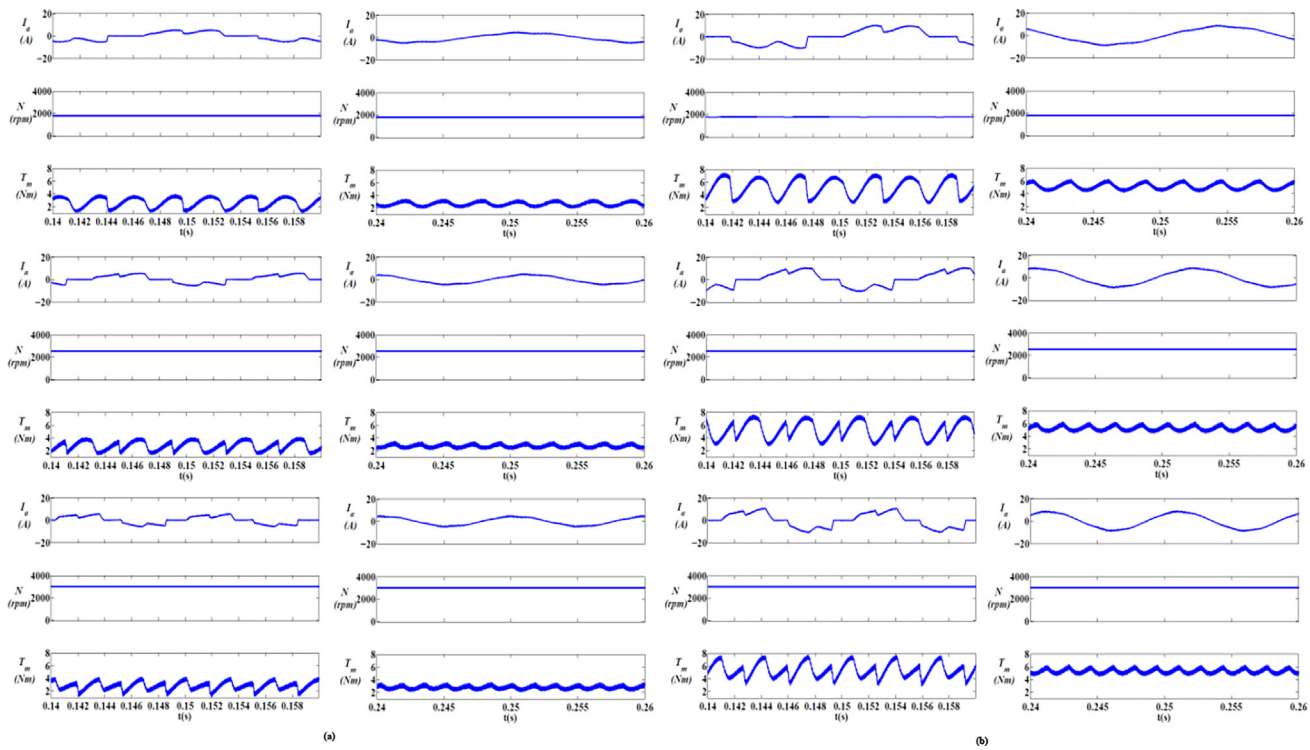

Fig. 7. Current, Speed and Torque comparison of BLDC motor with Conventional Six-step Control & MSPWM technique at a speed of 1750 rpm, 2500 rpm and 3000 rpm with (a) Load of 2.5 Nm (b) Load of 5 Nm.

Table 2
Torque ripple with MSPWM technique.

Speed (rpm) →	1750		2500		3000	
Load Torque (Nm) →	5	2.5	5	2.5	5	2.5
Torque ripple (Nm) →	2.5	1.6	2	1.3	1.8	1.2
Ripple factor →	0.5	0.64	0.4	0.52	0.36	0.48

Table 3
Torque ripple with conventional Six-step control.

Speed (rpm) →	1750		2500		3000	
Load Torque (Nm) →	5	2.5	5	2.5	5	2.5
Torque ripple (Nm) →	5.3	2.8	5	2.6	4.8	2.5
Ripple factor →	1.06	1.12	1	1.04	0.96	1

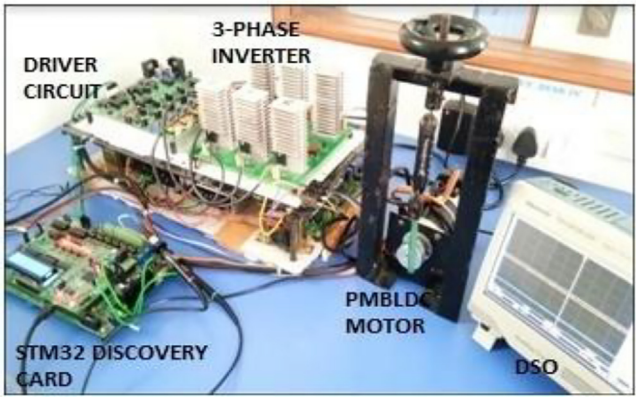

Fig. 8. Experimental setup photograph.

Table 4
BLDC motor Parameter.

Parameters	Values
Voltage (V)	36 V
Number of Poles (P)	4
Rated Speed (N)	4000 rpm
Rated Torque (Tm)	0.32 Nm
Per phase Resistance (r_s)	0.5 Ω
Per phase Inductance (Ls)	1.65 mH
Moment of inertia (J)	$17.3*10^{-6}$ kg-m^2
Torque Constant (Kt)	0.061 Nm/A

The conduction time is increased for a commanded speed of 1500 rpm. The experimental results proves that using presented MSPWM technique, sinusoidal stator currents are generated for a non-sinusoidal BLDC motor which helps in torque ripple reduction. As back emf being a function of rotor position and speed, it can be noted from Fig. 9(b) and Fig. 10(b), that the magnitude of back emf increases with increase in speed. With applied load changes the actual speed strictly follows the reference speed in Fig. 11(a), Fig. 12(a) and Fig. 13(a). The stator currents reacts according to the applied load. Fig. 11 (b), Fig. 12(b) and 13(b) shows the variation in load on the motor torque with the speed remaining constant. Small dips can be spotted in the speed curve with sudden load change when the motor operates at low speed about less than half the rated speed in Fig. 11(b) and Fig. 12(b). The variation in motor current and torque at a high speed of 3500 rpm with applied load change can be observed in Fig. 13(b). The PI controller takes about 300 ms to regain the set speed for speed below half the rated speed but takes a longer time to respond to the load disturbance and reach the set speed when the motor is operated at high speed of 3500 rpm. The torque and speed waveforms are smooth in nature with respect to the applied load changes. The stator current changes in accordance with the motor torque to meet the load demand.

This technique requires high speed processor as well as shaft encoder for instantaneous rotor position detection which makes the overall drive costly as compared to the conventional six-step operation. Since the proposed method controls motor operation in 3-phase conduction throughout the operation it may affect motor drive efficiency.

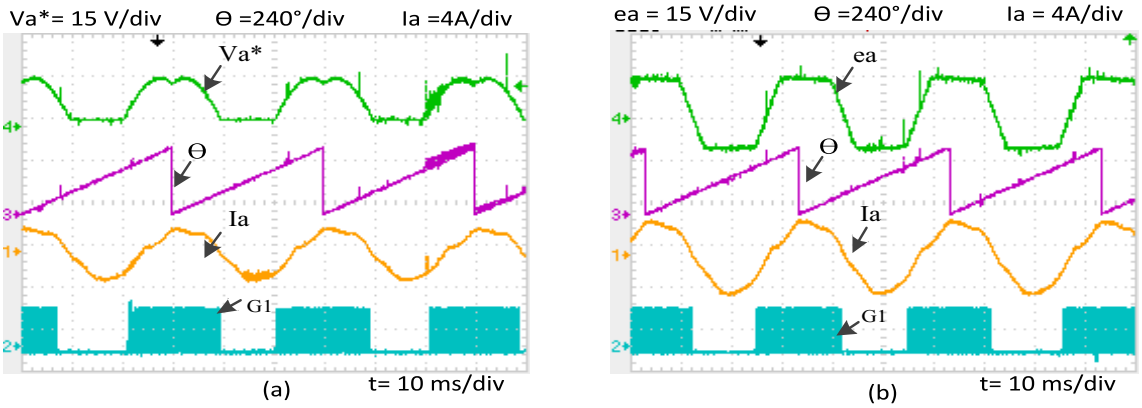

Fig. 9. Experimental waveforms of (a) modulating voltage, theta, phase current, gate pulses for switch S1 (b) back emf, theta, phase current, gate pulses for switch S1 with MSPWM technique at a speed of 1000 under full load condition.

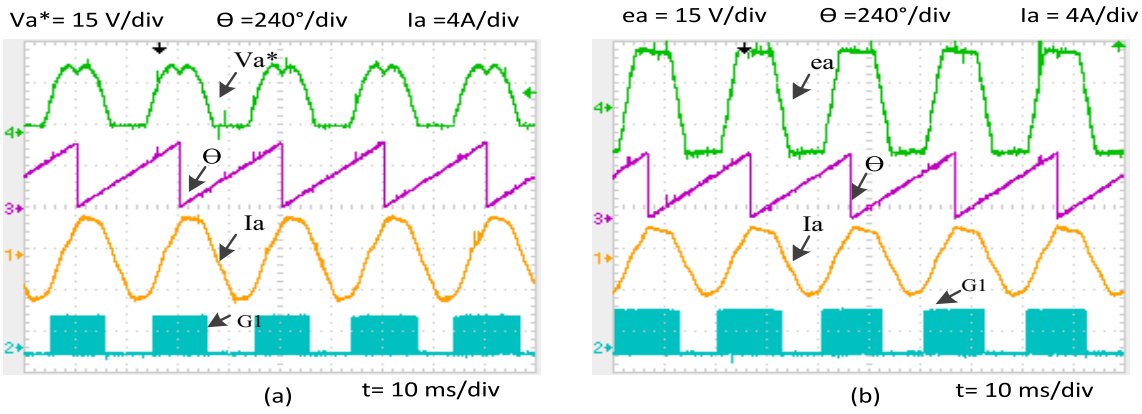

Fig. 10. Experimental waveforms of (a) modulating voltage, theta, phase current, gate pulses for switch S1 (b) back emf, theta, phase current, gate pulses for switch S1 with MSPWM technique at a speed of 1500 rpm under full load condition.

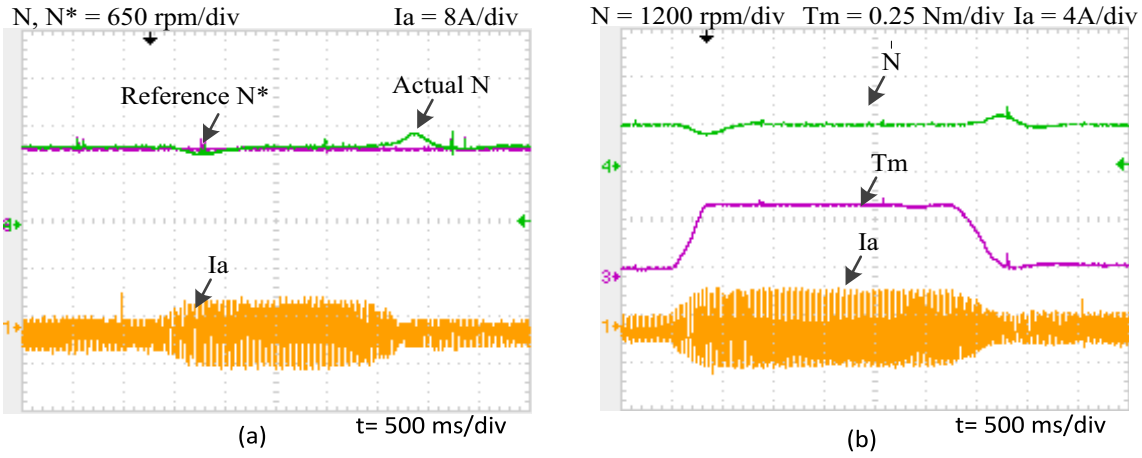

Fig. 11. Experimental waveforms of (a) comparison between actual speed and set speed, stator phase current with applied load change (b) behavior of actual motor speed, motor torque and stator phase current with applied load change at a speed of 1000 rpm.

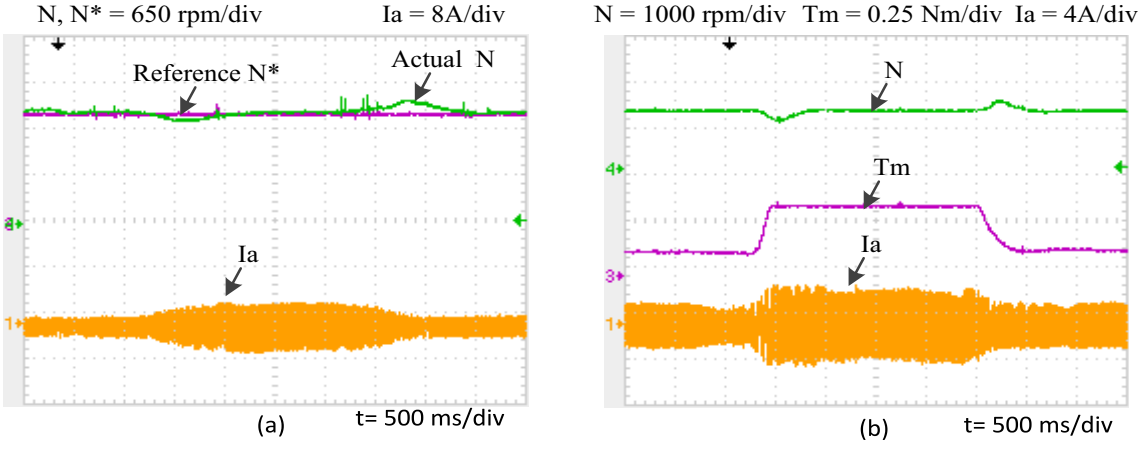

Fig. 12. Experimental waveforms of (a) comparison between actual speed and set speed, stator phase current with applied load change (b) actual motor speed, motor torque and stator phase current with applied load change at a speed of 1500 rpm.

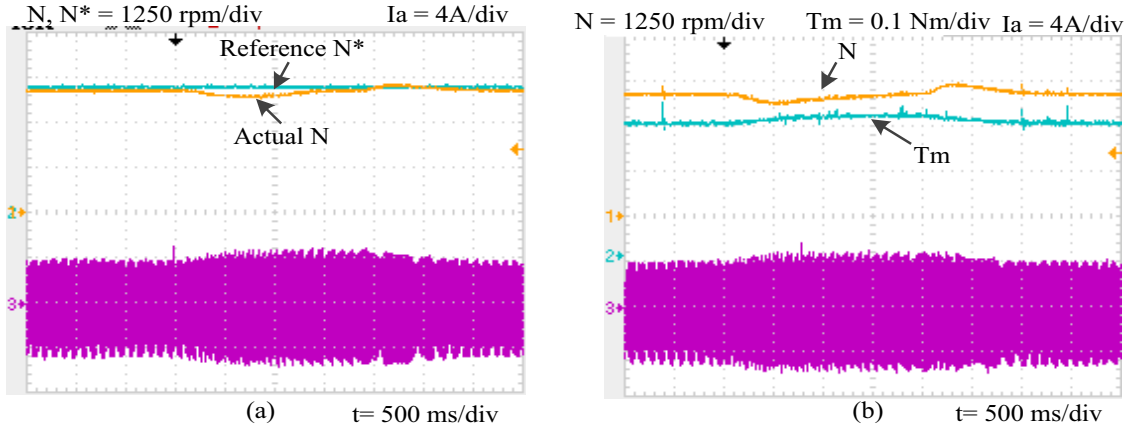

Fig. 13. Experimental waveforms of (a) comparison between actual speed and set speed, stator phase current with applied load change (b) actual motor speed, motor torque and stator phase current with applied load change at a speed of 3500 rpm.

5. Conclusion

This paper accord a simple closed-loop control technique of BLDC motor and torque ripple attenuation using sinusoidal excitation of phase winding with trapezoid back emf. The detailed analysis of Modified Sinusoidal Pulse Width Modulation (MSPWM) technique for closed-loop speed control of BLDC motor is discussed and simulation is performed to verify the performance of BLDC motor drive at different speed and load. The results are compared with widely used six-step control of BLDC motor. The better dynamic response is achieved and torque ripple is effectively reduced by the proposed method. The utilization of the DC link is also improved compared to conventional six-step control. The motor dynamic response is improved using only one PI controller as compared to the FOC and DTC techniques which reduces the control complexity. The proposed method is experimentally validated and dynamic performance of the drive with closed-loop speed control at wide range of speed and load is verified.

Declaration of Competing Interest

The authors declare that they have no known competing financial interests or personal relationships that could have appeared to influence the work reported in this paper.

References

[1] T.J.E. Miller, Brushless Permanent Magnet and Reluctance Motor Drives, Oxford Science Publication, UK, 1989.
[2] R. Krishnan, Electric Motor Drives: Modeling, Analysis, and Control, Prentice-Hall, Upper Saddle River, NJ, 2001.
[3] P. Pillay, R. Krishnan, Modeling, simulation, and analysis of permanent Magnet motor drives. Part II: The brushless dc motor drive, IEEE Trans. Ind. Appl. IA-25 (2) (1989) 274–279.
[4] Yanpeng Ji et al., Harmonic analysis on torque ripple of brushless DC motor based on advanced commutation control, J. Control Sci. Eng., Volume 2018, Article ID 3530127, 9 pages.
[5] D. Grenier et al., A Park-like transformation for the study and the control of a non sinusoidal brushless DC motor, IEEE Control Instrum. Ind. Electr. 2 (1995) 836–843.
[6] J. Holtz, On continuous control of PWM inverters in the over-modulation range including the six-step mode, IEEE Trans. on PE 8 (4) (1993) 546–553.
[7] A. Lidozzi et al., Vector Control of Trapezoidal Back-EMF PM Machines Using Pseudo-Park Transformation; IEEE Annual Power Electronics Specialists Conference; June 2008; DOI: 10.1109/PESC.2008.4592263.
[8] Lee et al., A comparison study of the commutation methods for the three-phase permanent magnet brushless DC motor; Paper presented in Electrical Manufacturing Technical Conference 2009: Electrical Manufacturing and Coil Winding Expo, EMCWA 2009; Nashville, TN; United States; pp. 49–55.
[9] Shucheng Wang, BLDC Ripple Torque Reduction via Modified Sinusoidal PWM, FAIRCHILD SEMICONDUCTOR POWER SEMINAR 2008–2009.
[10] J.R.B.A. Monteiro et al., Electromagnetic torque ripple and copper losses reduction in permanent magnet synchronous machines', Euro. Trans. Electr. Power (2011), https://doi.org/10.1002/etep.594.
[11] Z.Q. Zhu, et al. Flux-weakening characteristics of trapezoidal back-EMF machines in brushless DC and AC modes; 2006 CES/IEEE 5th Int. Power Electronics and Motion Control Conf., Shanghai China, 2006; vol. 2, pp. 1–5.
[12] A. Serpi et al., Design of flux-weakening space vector control algorithms for permanent magnet brushless DC machines on suitable synchronous reference frames, IET Electr. Syst. Transp. 9 (4) (2019) 215–225, https://doi.org/10.1049/iet-est.2018.5108.
[13] M. Bertoluzzo et al., Sinusoidal versus square-wave current supply of PM brushless DC drives: a convenience analysis, IEEE Trans. Ind. Electr. 62 (2015) 7339–7349.
[14] B. Tan et al., A new approach of minimizing commutation torque ripple for BLDCM, Energies 10 (2017) 1735, https://doi.org/10.3390/en10111735.
[15] Liu et al., Commutation-torque-ripple minimization in direct-torque-controlled PM brushless DC drives, IEEE Trans. Ind. Appl. 43 (2007) 1012–1021.
[16] C.K. Lad et al., Simple overlap angle control strategy for commutation torque ripple minimisation in BLDC motor drive, IET Electr. Power Appl. 12 (6) (2018) 797–807.
[17] Tao et al. Modeling simulation and experiment of permanent magnet brushless DC motor drive; Universities Power Engineering Conference, UPEC 2004; 39th International.
[18] D.C. Hanselman, Brushless Permanent Magnet Motor Design, Magna Physics Pub, 2006.
[19] P.C. Krause, O. Wasynczuk, S.D. Sudhoff, Analysis of Electric Machinery, IEEE Press, 1995.
[20] Z.G. Li, et al., Phase back EMF space vector oriented control of brushless DC motor for torque ripple minimization. In: Proceedings of the 2016 IEEE 8th International Power Electronics and Motion Control Conference, Hefei, China, 22–25 May 2016, pp. 2564–2570.